

Link between the hierarchy of fractional quantum Hall states and Haldane's conjecture for quantum spin chains

Masaaki Nakamura,¹ Emil J. Bergholtz,² and Juha Suorsa³

¹ *Department of Physics, Tokyo Institute of Technology, Tokyo 152-8551, Japan*

² *Max-Planck-Institut für Physik komplexer Systeme,
Nöthnitzer Straße 38, D-01187 Dresden, Germany*

³ *Department of Physics, University of Oslo, P.O. Box 1048 Blindern, 0316 Oslo, Norway*

(Dated: May 30, 2019)

We study a strong coupling expansion of the $\nu = 1/3$ fractional quantum Hall state away from the Tao-Thouless limit and show that the leading quantum fluctuations lead to an effective spin-1 Hamiltonian that lacks parity symmetry. By analyzing the energetics and discrete symmetries of low-lying excitations, we demonstrate that the $\nu = 1/3$ fractional quantum Hall state is adiabatically connected to both Haldane and large- D phases. This result indicates a close relation between the Haldane conjecture for spin chains and the fractional quantum Hall effect.

PACS numbers: 73.43.f, 73.43.Cd, 73.43.Nq, 75.10.Pq

I. INTRODUCTION

There are striking similarities between the catalogue of $SU(2)$ -symmetric quantum spin chains¹ and the hierarchy of fractional quantum Hall (FQH) states^{2,3,4,5}. Arguably the most striking parallel is that both systems allow a \mathbb{Z}_2 classification. Haldane conjectured¹ that half-integer $SU(2)$ quantum spin chains support gapless excitations, protected by a topological term in the effective action, while the integer spin chains develop a mass gap. A similar structure appears in the quantized FQH effect. At filling factors $\nu < 1$, quantized conductance plateaus only occur at rational ν with *odd* denominator, while in the vicinity of *even*-denominator fractions metallic behaviour is sustained. The Haldane conjecture and the phenomenology of the FQH effect communicate something pivotal about the low-lying excitations of seemingly disparate quantum phases, of low-dimensional magnetic materials and 2D electron gas in magnetic field. Hence, it is important to establish whether the similarities are merely accidental or if the structure of low-energy excitations in these systems have a related microscopic origin.

Already two decades ago, a more precise analogy between the two systems was discussed⁶ in terms of off-diagonal long-range order in FQH states⁷ and hidden orders present in $S = 1$ spin chains⁸ (see also Refs. 9,10,11 for related analogies). More recently it was realized that universal features of many quantum Hall (QH) phases can be understood on a microscopic level by studying the system on a thin torus^{12,13,14,15} (or Tao-Thouless, TT^{14,16,17}) limit. FQH states at odd-denominator fractions can be deformed into the TT limit without closing the energy gap, as has been established at all levels of rigor for the Laughlin fractions^{12,13,14,17,18,19} and to a high level of confidence for other fractions.^{14,15} Notably different behavior is found in states at even-denominator filling. For example, analysis of gapless QH state at filling fraction $\nu = 1/2$ shows that the system undergoes a first order quantum phase transition from a gapped

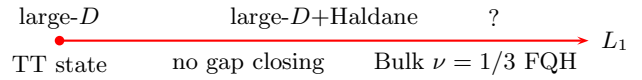


FIG. 1: (Color online) Phase diagram of $\nu = 1/3$ FQH system as a function of the circumference of the torus, L_1 . The TT limit, $L_1 \rightarrow 0$, of the FQH problem corresponds to the large- D phase of a spin-chain. By increasing L_1 , the bulk FQH state is adiabatically approached and the corresponding spin chain is, for intermediate L_1 , characterized by co-existing features of the large- D and Haldane phases. For very large L_1 the FQH/spin-chain correspondence cannot be derived microscopically as indicated by question mark on the spin-chain side of the phase diagram.

TT state to a gapless phase upon deformation of the torus.^{12,14} In fact, this analysis of the $\nu = 1/2$ FQH state uses a $S = 1/2$ spin chain description. A similar spin-chain picture²⁰ can also capture features of non-abelian states²¹, which further adds to the analogies between spin-chain physics and the FQH effect. The possibility of a relationship between the Haldane conjecture and the FQH effect was suggested in Ref. 12. In this article, we provide evidence for such a link by obtaining the phase diagram, sketched in Fig. 1, for the $\nu = 1/3$ FQH state away from the TT limit.

The rest of this article is organized as follows. In Section II we study the FQH system away from the TT limit and motivate a parity breaking spin-1 chain as an effective model of this system. In Section III we extend the effective spin-model to enable interpolation to more conventional spin models, which for example host large- D and Haldane phases. Concluding remarks are given in Section IV.

II. THIN TORUS LIMIT OF THE QUANTUM HALL SYSTEM

A. Mapping to one-dimensional model

We consider a model of N interacting electrons in the lowest Landau level on the torus. In the Landau gauge, a complete basis of N_ϕ degenerate single-particle states, labeled by $k = 0, \dots, N_\phi - 1$, can be chosen as

$$\psi_k(x) = (\pi^{1/2} L_1)^{-1/2} \sum_{n=-\infty}^{\infty} e^{i(k_1 + n L_2) x_1} e^{-\frac{1}{2}(x_2 + k_1 + n L_2)^2}, \quad (1)$$

where L_i are the circumferences of the torus, x_i the corresponding coordinates, and $k_1 = 2\pi k/L_1$ the momentum along the L_1 -cycle. We have set the magnetic length $l_B \equiv \sqrt{\hbar/eB}$ equal to unity. In this basis, any translation-invariant 2D two-body interaction Hamiltonian assumes the form

$$\mathcal{H} = \sum_{k>|m|} \hat{V}_{km}, \quad \hat{V}_{km} \equiv V_{km} \sum_i c_{i+m}^\dagger c_{i+k}^\dagger c_{i+m+k} c_i, \quad (2)$$

where the matrix-element V_{km} specifies the amplitude for a process where particles with separation $k+m$ hop m steps to a separation $k-m$ (note that m can be negative). At the filling $\nu = p/q$ the Hamiltonian commutes with the center-of-mass magnetic translations²² T_1 and T_2^q along the cycles, which implies, in particular, that the total momentum K along the L_1 -cycle is conserved modulo N_ϕ in this gauge.

Laughlin's state is an exact zero-energy eigenstate of the above Hamiltonian with the choice

$$V_{km} = (k^2 - m^2) e^{-2(k^2 + m^2)\pi^2/L_1^2} \quad (3)$$

obtained as the matrix elements of a periodized Haldane pseudo-potential $\nabla^2 \delta(\mathbf{r} - \mathbf{r}')$.^{3,23} The amplitudes V_{km} are exponentially damped in $1/L_1^2$. Therefore, at small L_1 the model can be approximated by a few most dominant terms such as \hat{V}_{10} , \hat{V}_{20} , \hat{V}_{21} , etc. We also study the model with Coulomb matrix elements where longer range electrostatic terms \hat{V}_{k0} are non-negligible.

B. Effective spin-1 model for $\nu = 1/3$

At the filling $\nu = N/N_\phi = 1/3$, the ground state manifold of the \hat{V}_{10} and \hat{V}_{20} -terms is three-fold degenerate, spanned by charge ordered states with one electron per a three-site unit cell: $|\dots 010 010 010 \dots\rangle$. The \hat{V}_{21} -term induces fluctuations upon these ground states through the process

$$|010 010\rangle \leftrightarrow |001 100\rangle. \quad (4)$$

The truncated model can be mapped to an $S = 1$ quantum spin chain by identifying the states of the unit cell as

$|010\rangle \rightarrow |0\rangle$, $|001\rangle \rightarrow |+\rangle$, and $|100\rangle \rightarrow |-\rangle$. Clearly the identification explicitly break translational symmetry—there are three equivalent ways of grouping three electronic sites into one spin site. By choosing a particular grouping of the sites (so that the ground state appears at total $S^z = 0$) we effectively mod out the original three-fold degeneracy.²⁴ In terms of $S = 1$ variables, the \hat{V}_{21} -process is then accounted for by the Hamiltonian $\mathcal{H} = \sum_{i=1}^N h_{i,i+1}$ with

$$h_{ij} = \frac{1}{2} S_i^+ S_j^- (1 - (S_i^z)^2) (1 - (S_j^z)^2) + \text{H.c.} \quad (5)$$

We note that this Hamiltonian does not have the space inversion and spin reversal symmetries: the process $|00\rangle \leftrightarrow |+-\rangle$ exists but $|00\rangle \leftrightarrow |-+\rangle$ does not. This “parity” breaking is a consequence of the dependence of V_{km} on the single-particle momentum transfer m . For a fixed (initial) separation $k+m$, the amplitudes are asymmetric with respect to $m \leftrightarrow -m$. Inward hops have a greater amplitude than outward hops.

In the TT limit, the fractionalized excitations of the system are domain walls between the degenerate vacua. These can be included in the effective spin-chain description by introducing at the domain walls edge spins that carry a lower, $S = 1/2$, representation. The energetics of spatially separated domain walls are not essential to the FQH phenomenology as long as we can assume them to localize. Hence, in this paper we only analyze the exciton (bound quasielectron-quasihole pair) gap, which we relate to the Haldane gap in the effective spin model.

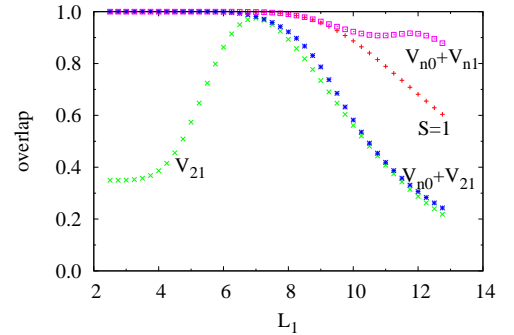


FIG. 2: (Color online) Overlaps of the exact $N = 8$ Laughlin state with the ground states of truncated Hamiltonians, consisting of a few leading terms, as functions of L_1 . Also shown is the projection of the exact Laughlin state onto $S = 1$ -chain Hilbert space.

To study the relevance of the model (5) for the Laughlin state, we have analyzed ground state overlaps and excitation spectra. Fig. 2 shows as functions of L_1 the overlaps of the exact Laughlin state, obtained as the ground state of the Hamiltonian including all \hat{V}_{km} terms, with the ground states of various truncations: \hat{V}_{21} , $\sum_n \hat{V}_{n0} + \hat{V}_{21}$, $\sum_n (\hat{V}_{n0} + \hat{V}_{n1})$. Also, the projection of the

Laughlin state onto the Hilbert space of $S = 1$ chain is shown.

The high overlap with the \hat{V}_{21} Hamiltonian at around $L_1 = 7$ indicates that the ground state around this L_1 is related to the ground state of the \hat{V}_{21} -Hamiltonian, which when restricted to the $S = 1$ -chain Hilbert space, maps to the parity-broken $S = 1$ model in (5). Further evidence comes from the fact that the truncated Hamiltonian reproduces the low-energy part of the entanglement spectrum of the Laughlin state²⁵.

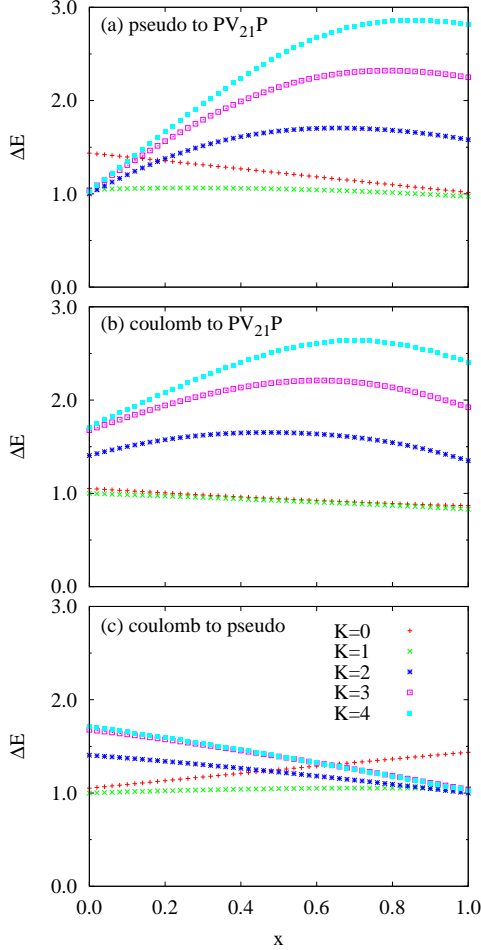


FIG. 3: (Color online) Excitation spectra (the lowest levels for each K) of the Hamiltonians (a) $\mathcal{H} = (1-x)\mathcal{H}_p + x\mathcal{P}\hat{V}_{21}\mathcal{P}$, (b) $\mathcal{H} = (1-x)\mathcal{H}_c + x\mathcal{P}\hat{V}_{21}\mathcal{P}$, and (c) $\mathcal{H} = (1-x)\mathcal{H}_c + x\mathcal{H}_p$, for fixed $L_1 = 7$ and $N = 8$.

To determine whether the low-lying excitations are also captured by a $S = 1$ spin chain, we study how the spectrum of the quantum Hall system changes as we deform the potential from the full exact pseudopotential and Coulomb potential to $\mathcal{P}\hat{V}_{21}\mathcal{P}$, where the projector \mathcal{P} projects to the Hilbert space of the $S = 1$ chain. Note that the pure hopping Hamiltonian \hat{V}_{21} preserves $S = 1$ Hilbert space in the ground state sector, in which the TT state lies, but in general this is not true. For example,

		\mathcal{P}	\mathcal{T}	k	BC	M
E_0	G.S.	+1	+1	0	+1	0
E_1	Haldane	-1	-1	0	-1	0
E_2	large- D	+1	+1	0	-1	0
E_3	dimer	+1	+1	π	-1	0
E_4	XY	+1	*	0	+1	2

TABLE I: Discrete symmetries of the excitation spectra (\mathcal{P} : space inversion, \mathcal{T} : spin reversal, k : wave number, and M : total S^z). BC=1 (BC=-1) stands for (anti)periodic boundary conditions. G.S. means the ground state.

\hat{V}_{21} acting on 100 100 takes it to a configuration 011 000, which lies outside the $S = 1$ Hilbert space. Hence, we include the projectors to make connection to the spin-chain models. Results of the analysis are shown in Fig. 3, where we have fixed $L_1 = 7$. The panels show how the spectrum of lowest-lying excitations in each K -sector changes upon various linear interpolations: (a) full Coulomb Hamiltonian \mathcal{H}_c to $\mathcal{P}\hat{V}_{21}\mathcal{P}$, (b) \mathcal{H}_c to the Haldane pseudopotential Hamiltonian \mathcal{H}_p , and (c) \mathcal{H}_p to $\mathcal{P}\hat{V}_{21}\mathcal{P}$. According to the discussion above our results provide an explicit interpolation between the FQH Hamiltonian (2) and the spin chain defined in (5).²⁶ We observe that the gap remains finite and approximately constant throughout the interpolations. The ordering of the levels as a function of the momentum K (relative to the ground state) can be thought of as the exciton dispersion. We find that the dispersions obtained with the Coulomb and the $\mathcal{P}\hat{V}_{21}\mathcal{P}$ Hamiltonians largely agree. It is interesting to note that the low-lying $K = 0$ excitation crosses some of the finite- K levels upon deformation of the Coulomb to the pseudopotential Hamiltonian. For the purpose of the present article we conclude that also the spectrum of our spin model is compatible with that of the FQH problem for a realistic interaction.

III. ANALYSIS OF THE SPIN MODEL

A. Twisted boundary method for ground state

In order to identify the universality class of the ground state of the model (5), we extend the Hamiltonian as

$$h_{ij} = \frac{1}{2} S_i^+ S_j^- (1 - \lambda (S_i^z)^2) (1 - \lambda (S_j^z)^2) + \text{H.c.} \\ + \Delta S_i^z S_j^z + \frac{D}{2} ((S_i^z)^2 + (S_j^z)^2). \quad (6)$$

We then study the adiabaticity of deformations from parameter regions where physical properties are already known, to the point $\Delta = D = 0$ and $\lambda = 1$, which is related to the $\nu = 1/3$ FQH problem according to the discussion above, and will henceforth be referred to as the FQH point.

Now let us review properties of this model (6) for already known parameter regions. For $\lambda = D = 0$,

this model becomes the $S = 1$ XXZ spin chain. Then the system becomes ferromagnetic ($\Delta < 0$), XY phase ($-1 \leq \Delta \leq 0$), Haldane phase ($0 < \Delta < \Delta_c$), and Néel state ($\Delta_c < \Delta$), where $\Delta_c = 1.17 \pm 0.02$.²⁷ The XY-Haldane transition is of the Berezinskii-Kosterlitz-Thouless (BKT) type reflecting the $SU(2)$ symmetry of the XY model.^{28,29} For $\lambda = 0$, with finite D and Δ , phase diagram has been obtained using the level-crossing method with twist boundary conditions.^{29,30} For example, at $\Delta = 1$, a phase transition from Haldane to large- D phases takes place at $D_c = 0.968 \pm 0.001$.^{33,34,35}

In order to analyze the parameter regions beyond the known ones, we analyze the excitation spectra of the system under antiperiodic boundary conditions using the exact diagonalization.^{29,30} The antiperiodic boundary conditions have the role of *making the non-degenerate ground states artificially two-fold degenerate*. In such analysis, there are four essential excitations that can be used to identify four possible phases. By probing the differences

$$\Delta E_i \equiv E_i - E_0, \quad (i = 1, 2, 3, 4) \quad (7)$$

where E_0 is the ground state energy with periodic boundary conditions, the ground state of the infinite-size system can be identified according to the lowest excitation in finite-size systems. This means that phase transition points are given by level crossings of the two lowest energy levels under the twisted boundary conditions.

Discrete symmetry plays an important role in relating the twisted levels to four physical phases (XY, Haldane, large- D , and dimer phases). According to the valence-bond-solid pictures³¹ and periodicity, the three gapped states under twisted boundary conditions are classified by space inversion ($\mathcal{P} : S_i^\alpha \rightarrow S_{L+1-i}^\alpha$), spin reversal ($\mathcal{T} : S_i^\alpha \rightarrow -S_i^\alpha$),²⁷ and translational ($e^{ik} : S_i^\alpha \rightarrow S_{i+1}^\alpha$)³² symmetries as summarized in Table I. In the present system, the spin-reversal symmetry is always synchronized

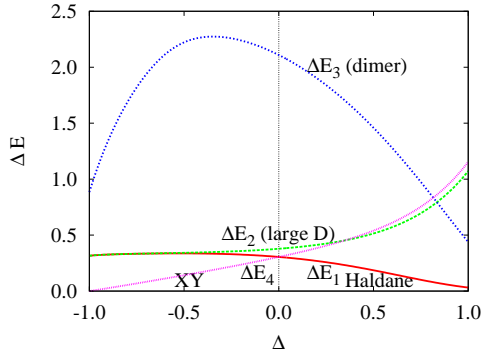


FIG. 4: (Color online) Excitation spectra ΔE_i of the XXZ chain ($D = \lambda = 0$) with system size $N = 16$ under antiperiodic boundary conditions. The lowest spectrum corresponds to different four ground states (XY, Haldane, large- D , and dimer phases). A level crossing at $\Delta = 0$ corresponds to XY-Haldane phase transition point reflecting the hidden $SU(2)$ symmetry.^{28,29}

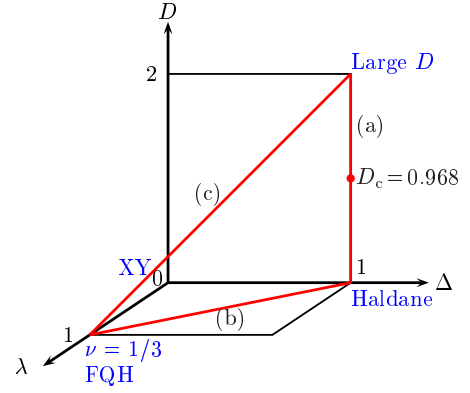


FIG. 5: (Color online) Parameter space of the model (6) connecting three phases (XY, Haldane, large- D phases) in the $S = 1$ quantum spin chain and the $\nu = 1/3$ fractional quantum Hall state.

with the space-inversion symmetry, hence we refer to them as parity. The important role of twisted boundary conditions should be noted here; *under periodic boundary conditions the three gapped states have the same parity*. In this method, finite-size effects are extremely small even in small size clusters, since the positions of the level-crossing points are free from logarithmic corrections. For example, in case of the $S = 1$ XXZ model ($D = \lambda = 0$), there is a level-crossing point between ΔE_1 and ΔE_4 at $\Delta = 0$, which corresponds to the BKT-type transition between the XY and the Haldane phases (see Fig. 4).²⁹

According to the conventional classification, the gapped state at the FQH point ($\Delta = D = 0, \lambda = 1$) would be expected to belong either to the Haldane or large- D phases. Therefore, we consider the behavior of the excitation spectra along the following three paths in the parameter space (see Fig. 5): (a) $\Delta = 1, \lambda = 0$, (b) $\Delta = 1 - \lambda, D = 0$, and (c) $\Delta = 1 - \lambda, D = 2(1 - \lambda)$. According to the numerical data of the excitation energies obtained by the exact diagonalization of $N = 16$ clusters, there is a phase transition between Haldane and large- D phases in path (a). On the other hand, there is no level-crossing point between the lowest two spectra in the path (b) and (c), so that the FQH point is adiabatically connected from both Haldane and large- D phases (see Fig. 6).

The absence of phase transitions can be understood in terms of the discrete symmetry of the system. In the excitation spectra along the path (a) with finite $\lambda > 0$, the level crossing between ΔE_1 and ΔE_2 is absent as shown in Fig. 7(a). This is because there are finite matrix elements between two parity sectors that were independent in parity-invariant case, and these two energy levels hybridizes. Therefore absence of the level-crossing is due to the parity symmetry breaking. Thus the FQH state ($\Delta = D = 0, \lambda = 1$) belongs to both Haldane and large- D phases. This situation is quite similar to the absence of phase transition between dimer and large- D phases in

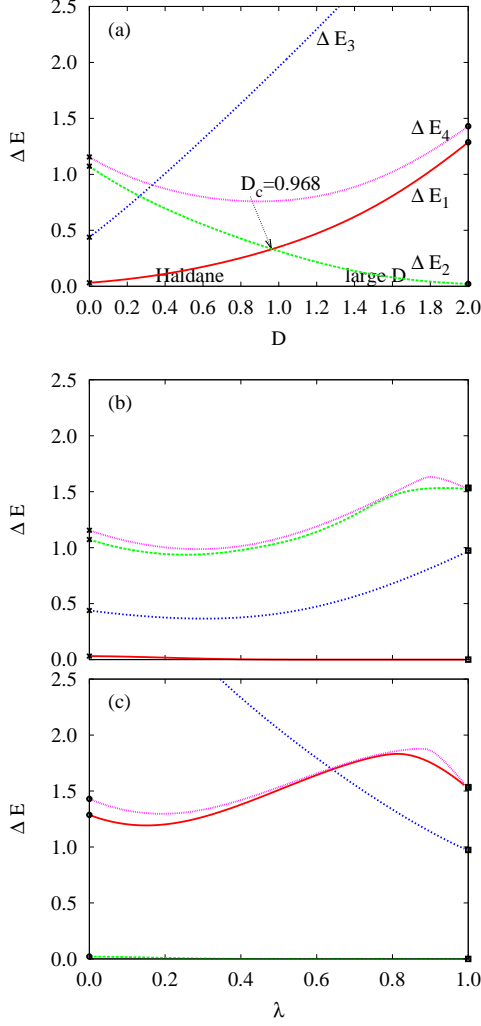


FIG. 6: (Color online) Excitation spectra of the $N = 16$ system under antiperiodic boundary conditions along the paths (a), (b), and (c) of Fig. 5. In path (a), a level crossing between different parity (ΔE_1 and ΔE_2) corresponds to the phase transition point between the Haldane and large- D phases at $D_c = 0.968 \pm 0.001$.³⁵ In paths (b) and (c), there are no gap closing points, since there are no level-crossing points between the lowest two excitations.

the $S = 1$ bond-alternating Heisenberg chain with finite D .^{33,35}

$$h_{ij} = [1 + \delta(-1)^i] \mathbf{S}_i \cdot \mathbf{S}_j + \frac{D}{2} ((S_i^z)^2 + (S_j^z)^2). \quad (8)$$

In this case, a similar level repulsion takes place between E_2 and E_3 due to the breaking of the translational symmetry (see Fig. 7(b)). An argument for the stability of the Haldane gap state in terms of symmetry has also been discussed in Ref. 36.

B. Energy gap

Let us turn our attention to the behavior of the energy gap for $S^z = 0$ and $S^z = 1$ excitations in paths (b) and (c) of Fig. 5. The energy gaps are obtained by the following extrapolation function $\Delta E_g(N) = \Delta E_g(\infty) + A/N + B/N^2$ using the data of the system size $N = 8, 10, 12, 14, 16$. Especially, for the $S^z = 0$ case, extrapolation of difference between the lowest two excitation energies under the twisted boundary conditions ($\Delta E_{1,2,3}$) gives the energy gap with good accuracy.³⁷ We have checked the validity of our analysis by comparing our result with the known value of the Haldane gap $E_g(\infty) = 0.4104 \dots$. In Fig. 8, the energy gaps along path (b) and (c) are shown. Energy gap for $S^z = 2$ which has been omitted is always larger than that of $S^z = 1$. As we expected, there is no gap closing point in both paths. In path (b), the Haldane gap is given by $S^z = 0$ gap, and there is a level-crossing in the excited state close to the FQH point ($\lambda = 1$), then the $S^z = 1$ state gives the energy gap. In this sense our $S = 1$ model actually give closer description of the $\nu = 1/3$ Coulomb state than the the pseudopotential interaction (which has the Laughlin state as its exact ground state) since the energy gap of the 1D mapped Coulomb interaction has $K = 1$ ($S^z = 1$) energy gap, while the pseudopotential interactions has a

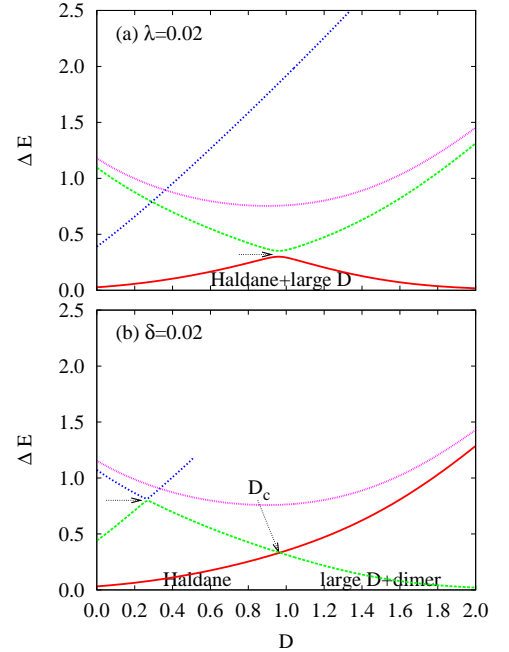


FIG. 7: (Color online) Excitation spectra with system size $N = 16$ around the path (a) of Fig. 5 with (a) finite $\lambda = 0.02$ and (b) $\delta = 0.02$ (bond alternation). In (a), a level repulsion appears between two spectra ΔE_1 and ΔE_2 due to the breaking of parity symmetry, while in (b) ΔE_1 and ΔE_3 hybridize due to the breaking of translational symmetry.

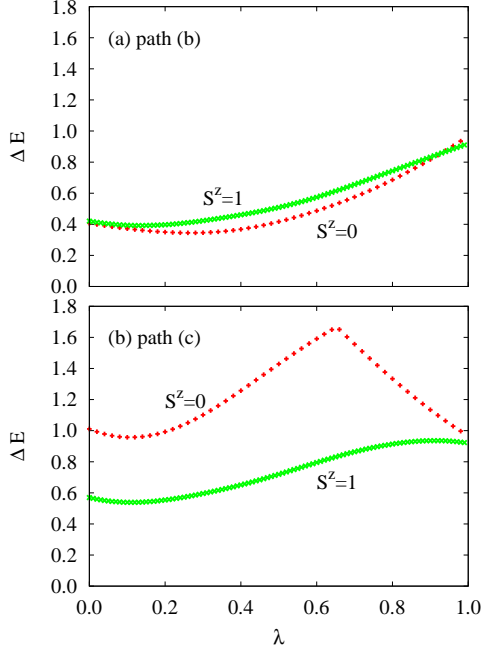


FIG. 8: (Color online) Extrapolated energy gap for $S^z = 0$ and 1 along the paths (b) and (c) of Fig. 5. In path (c), there is a level crossing in excited states. At the FQH state ($\lambda = 1$), $S^z = 1$ gap is the lowest which is consistent with the structure of the excited states with Coulomb interactions.

minimal gap in the $K = 2$ ($S^z = 2$) sector.

C. Order parameter

In addition to the analysis of energy spectra, we consider behavior of the string order parameter (SOP),⁸

$$\mathcal{O}^\alpha = - \lim_{|k-l| \rightarrow \infty} \left\langle S_k^\alpha \exp \left[i\pi \sum_{j=k+1}^{l-1} S_j^\alpha \right] S_l^\alpha \right\rangle, \quad (9)$$

where $\langle \dots \rangle$ means the ground-state expectation value, and $\alpha = x, y, z$. We calculate \mathcal{O}^z in finite-size systems with $l = k + L/2$ in the three paths (a)-(c) (see Fig. 6) It is difficult to identify the phase transition point from the data of the small clusters, due to the large finite-size effect, but the SOP tends to vanish at the large- D and the FQH state. Thus, in the sense of the SOP, the FQH point is more closely related to the large- D phase than to the Haldane phase. However, there are certainly string order like correlations in the ground state at the FQH point: only the configurations $|00\rangle, |0+\rangle, |-0\rangle$ and $|+-\rangle$ can appear, but never $|-+\rangle, |--\rangle$ or $++\rangle$. Therefore, the ground-state wave function always includes the hidden antiferromagnetic order such as $|+-+ -00+ -0+ - \dots\rangle$ which is detected by the SOP. That these correlations are not visible in our extrapolation for the SOP appear to be

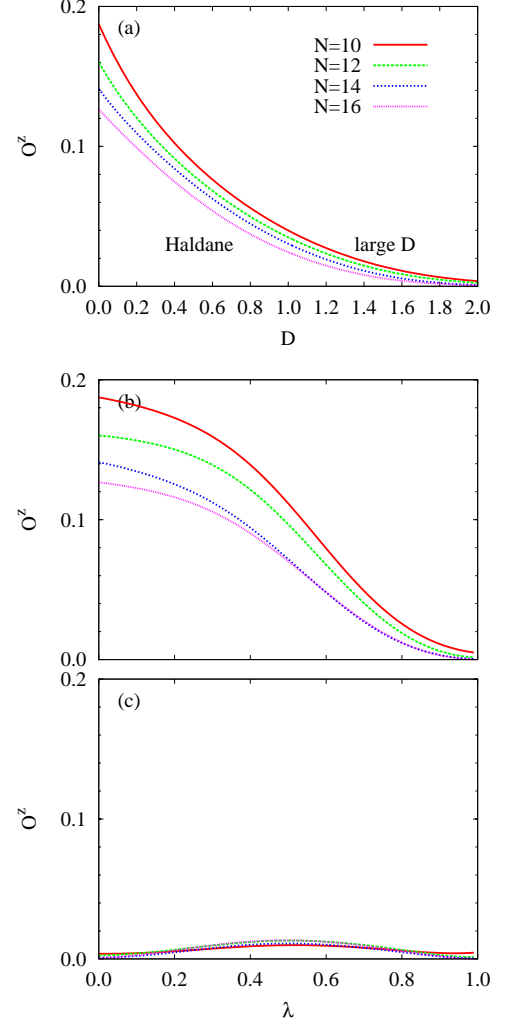


FIG. 9: (Color online) String order parameter \mathcal{O}^z with $N = 10-16$, along the paths (a), (b), and (c) (see Fig. 5). The SOP tends to vanish around the large- D phase and the FQH state.

because of their insufficient weight in the ground state wave function.

IV. CONCLUSION

In conclusion, we have discussed the $\nu = 1/3$ FQH state by one-dimensional mapping around the TT limit. In TT limit, the system is charge-ordered state which corresponds to the large- D phase of the $S = 1$ spin chain. Then away from the TT limit, the system still has characteristics of the large- D phase, but the Haldane phase also coexists due to the broken parity symmetry. It is plausible that the features of the Haldane state may further increase as the circumference of the torus L_1 is increased beyond the range where our analysis is applicable (see Fig. 1). This scenario also receive circumstantial sup-

port by the observation in Ref. 6 that the off diagonal long range order in the Laughlin state is very similar in nature to the string order in the Haldane phase.

The present analysis may also be extended to general odd denominator filling fractions, ν , by mapping to integer- S spin chains. It is well known that the both the gapped Haldane and large- D phases only exists for odd integer spin chains, and the present work signals their relevance to the odd denominator rule in the hierarchy of fractional quantum Hall states.

V. ACKNOWLEDGMENTS

We acknowledge many discussions with K. Hida, A. Karlhede, H. Nakano, K. Okamoto, M. Oshikawa, and S. Ryu. M. N. acknowledges the visitors program at the Max-Planck-Institut für Physik komplexer Systeme, Dresden, Germany, and support from Global Center of Excellence Program “Nanoscience and Quantum Physics” of the Tokyo Institute of Technology by MEXT.

-
- ¹ F. D. M. Haldane, Phys. Lett. **93A**, 464 (1983); Phys. Rev. Lett. **50**, 1153 (1983).
 - ² R. B. Laughlin, Phys. Rev. Lett. **50**, 1395 (1983).
 - ³ F. D. M. Haldane, Phys. Rev. Lett. **51**, 605 (1983).
 - ⁴ B. I. Halperin, Phys. Rev. Lett. **52**, 1583, 2390(E) (1984).
 - ⁵ J. K. Jain, Phys. Rev. Lett. **63**, 199 (1989).
 - ⁶ S. M. Girvin and D. P. Arovas, Physica Scripta. T **27**, 156-159, (1989).
 - ⁷ S. M. Girvin and A. H. MacDonald, Phys. Rev. Lett. **58**, 1252 (1987).
 - ⁸ M. den Nijs and K. Rommelse, Phys. Rev. B **40**, 4709 (1989).
 - ⁹ D. P. Arovas, A. Auerbach, and F. D. M. Haldane, Phys. Rev. Lett. **60**, 531 (1988).
 - ¹⁰ Z. Nussinov and G. Ortiz, Ann. Phys. (N.Y.) **324**, 977 (2009).
 - ¹¹ D. P. Arovas, K. Hasebe, X.-L. Qi, and S.-C. Zhang, Phys. Rev. B **79**, 224404 (2009).
 - ¹² E. J. Bergholtz and A. Karlhede, Phys. Rev. Lett. **94**, 026802 (2005).
 - ¹³ A. Seidel, H. Fu, D. -H. Lee, J. M. Leinaas, and J. Moore, Phys. Rev. Lett. **95**, 266405 (2005).
 - ¹⁴ E. J. Bergholtz and A. Karlhede, J. Stat. Mech. L04001 (2006); Phys. Rev. B **77**, 155308 (2008).
 - ¹⁵ E. J. Bergholtz, T. H. Hansson, M. Hermanns, and A. Karlhede, Phys. Rev. Lett. **99**, 256803 (2007).
 - ¹⁶ R. Tao and D. J. Thouless, Phys. Rev. B **28**, 1142 (1983).
 - ¹⁷ P. W. Anderson, Phys. Rev. B **28**, 2264 (1983).
 - ¹⁸ S. Jansen, E. H. Lieb, and R. Seiler, Commun. Math. Phys. **285**, 503 (2009).
 - ¹⁹ E. H. Rezayi and F. D. M. Haldane, Phys. Rev. B **50**, 17199 (1994).
 - ²⁰ E. Wikberg, E. J. Bergholtz, and A. Karlhede, J. Stat. Mech. P07038 (2009).
 - ²¹ G. Moore, and N. Read, Nucl. Phys. B **360**, 362 (1991).
 - ²² F. D. M. Haldane, Phys. Rev. B **31**, 2529 (1985).
 - ²³ S. A. Trugman and S. A. Kivelson, Phys. Rev. B **31**, 5280 (1985).
 - ²⁴ One might worry that the three-fold degeneracy of the TT state would cause trouble as they would map onto three different spin configurations for each of the three groupings into spin sites. However, these states are not connected by the Hamiltonian as the correspond to different K -values, hence it does make sense to define one spin subspace corresponding to each of the three degenerate ground states (and their respective low energy excitations).
 - ²⁵ A. M. Lauchli *et al*, in preparation.
 - ²⁶ The projection does nothing to the ground state but affects the excited states.
 - ²⁷ A. Kitazawa and K. Nomura, J. Phys. Soc. Jpn. **66**, 3944 (1997); 3379 (1997), and references therein.
 - ²⁸ A. Kitazawa, K. Hijii, and K. Nomura, J. Phys. A: Math. Gen. **36**, L351 (2003).
 - ²⁹ K. Nomura and A. Kitazawa, J. Phys. A: Math. Gen. **31**, 7341 (1998).
 - ³⁰ A. Kitazawa, J. Phys. A **30**, L285 (1997).
 - ³¹ I. Affleck, T. Kennedy, E. Lieb, and H. Tasaki, Phys. Rev. Lett. **59**, 799 (1987); Commun. Math. Phys. **115**, 477 (1988).
 - ³² Large- D and dimer states can be classified by the wave number due to difference of the periodicity.
 - ³³ W. Chen, K. Hida, and B. C. Sanctuary, J. Phys. Soc. Jpn. **69**, 237 (2000).
 - ³⁴ W. Chen, K. Hida, and B. C. Sanctuary, Phys. Rev. B **67**, 104401 (2003).
 - ³⁵ W. Chen, K. Hida, and B. C. Sanctuary, J. Phys. Soc. Jpn. **77**, 118001 (2008).
 - ³⁶ Z.-C. Gu and X.-G. Wen, arXiv:0903.1069 (2009).
 - ³⁷ H. Nakano and A. Terai, J. Phys. Soc. Jpn. **78**, 014003 (2009).